A Fast and Simple Machine Vision Framework for Approximating the Volume of Axi-Symmetric Objects Using Shadow Ray Casting

Siwakorn Sukprasertchai, Taweepol Suesut*, and Navaphattra Nunak
School of Engineering, King Mongkut's Institute of Technology Ladkrabang, Bangkok, Thailand
Email: siwakorn.su@ku.th (S.S.), taweepol.su@kmitl.ac.th (T.S.), navaphattra.nu@kmitl.ac.th (N.N.)

***Abstract*—The volume measurement using machine vision system is contactless techniques that play an important role in industries now a day. Basically, three-dimensional reconstruction is required to determine a depth using a special lighting system or multiple cameras. This increases the complexity of the measurement system. A fast and simple machine vision framework called RayVol for estimating the volume of axisymmetric objects in near real-time using a single camera and simple illumination is presented. The RayVol framework employs a shadow casting method to reconstruct the 3D shape of the object by tracing rays from the object's shadow pixels to the light source location. The result of this technique shows a significant accuracy improvement from the area-projection method. A virtual slice representing the cross-section of an object is reconstructed using a cubic spline approximation from baseline points derived from the boundary pixels of the object image and a shadow casting method. The volume estimation was calculated by restricted integration using the Riemann sum estimation algorithm, and the closed area of the virtual slices was calculated using the shoestring algorithm. Mangoes were used as a case study of the RayVol framework. The volume estimation provides the correlation coefficient of 0.9849 between the developed system and the water replacement method.**

***Index Terms*—3D reconstruction, non-contact volume approximation, shadow casting**

I. Introduction

Currently, the development of industrial production processes has been emphasized on both qualitative and quantitative aspects. Size inspection is an important process for various industries such as fruit and vegetable grading by evaluating volume, length, and weight. Completeness inspection, sizing and grading are considered important steps in production to produce products that meet the needs of customers. Today, inspection and classification using machine vision systems is widely used due to being able to work accurately and quickly, it is also a non-destructive and non-contact inspection. This greatly reduces cross-contamination into the product. Especially food and agricultural products that need to be hygienic production process.

Physical attributes such as volume, mass, surface area, and geometric mean diameter (GMD) are commonly used for sorting, grading, packaging, pesticide applications, and more especially fresh fruits [1]. Among these attributes, mass and volume are the most frequently used for size classification. Sizing by weight is typically achieved by converting gravitational force from mechanical mechanisms to measurable data using a force transducer, such as a load cell, integrated with conveyor belts, and performed as in-motion or dynamic weighing. Such systems are capable of measuring weight at around a hundred per minute. However, due to the electro-mechanical structure of these systems, several factors such as vibration, dust, temperature fluctuations, electrical noise, and corrosion can affect their accuracy. Additionally, recalibration or zero resets are required after a certain period of usage to maintain precision [2].

Since mass and volume are related to density, it might be possible to determine the weight from volume by using a pre-determined density [3]. Volume is determined by the spatial size of an object in three dimensions, and estimating this requires three-dimensional information. One of the most straightforward, simple, and accurate methods of estimating volume is based on Archimedes' Principle, which determines the amount of fluid medium displaced by an object [4]. An alternative technique based on medium change is the use of an acoustic method, whereby a known-size closed chamber with a speaker is excited by an oscillating signal. The amplitude of sound generated from the speaker varies due to a change in the air volume inside the chamber [5–8]. However, such processes must be done with offline process, and manually taking a sample has led to a risk of damaging a sample. Furthermore, when dealing with in-line conveyor belts, the measuring time is a major key issue, making this method unsuitable for use in an in-line process.

An alternative approach is machine vision, a non-contact, rapid, and non-destructive measuring technique. In recent years, this approach has gained dominance in many agricultural processing systems [9]. As mentioned earlier, three-dimensional information is required to estimate the volume. Such a system is called a range imaging system or 3D scanner system.

Manuscript received September 13, 2023; revised October 29, 2023; accepted November 7, 2023.
*Corresponding author

doi: 10.18178/ijeetc.13.2.176-183

The 3D scanner method requires an energy-emitting source as an additional component to project energy onto an inspected object. The most common implementations are based on time-of-flight (TOF) and triangulation principles; such systems have gained a lot of traction in recent decades. The simple active system is laser triangulation [10–13], a light source such as laser strip line is utilized, projecting onto an object, the reflected laser strip line is detected by a camera frame by frame, in sync with the conveyor belt position while it is still moving. During this process, an analysis of the distortions of the laser strip line is performed to obtain the depth information, and then 3D information of the object is reconstructed. This technique requires many frames to be fully completed in 3D reconstruction, which is time-consuming. The triangulation principle with a simultaneously reconstructed capability by using an RGB-D computer vision system to reconstruct the 3D shape for volume estimation was published by [14, 15]. They used PrimeSense Camine 1.09, an RGB-D commercial camera system (RGB-D stands for an RGB camera with a depth acquisition system) for an acquisition system. The projected light pattern is then distorted by the spatial object profile and detected by the camera. This system has the capability of simultaneously reconstructing 3D information in a single frame. A fully completed 3D model is used to estimate the volume by integrating pixel values along the length axis. Another technique has been simultaneous 3D reconstruction capability using the TOF principle [16], which has a more complex system compared to triangulation based. There are some publications that used TOF camera [1, 17], the Microsoft Kinect V2.0, a commercial low-cost RGB-D camera system. This TOF camera used a pulsed light method, simultaneously rebuilding the 3-D model which was analyzed and extracted. These publications have demonstrated that the active principle returns high accuracy with robustness and real-time capability.

From a deterministic point of view, rapid measuring with simple techniques while still being cost-effective is a challenging task. Since most fresh products presumably have axi-symmetric shapes and might be fitted to the common 3D mathematical shapes: ellipsoid, spheroid, paraboloid, and more. From this assumption, there are many techniques developed by researchers that are related by mathematical models and numerical analysis. There are many published [18–24], using only top view image which acquired from single 2D computer vision to extracted maximum width and height of object to estimate whole volume from mathematic model. Some researchers used disk methods to improve the accuracy, by slicing the material as virtual slices. The object volume is estimated by the integration of the area of each slice, where area is computed from mathematical model or interpolation that derived from width and height from top-view image [25–28]. However, predictions based on 2D information lack actual surface depth distribution [29], and there are also some fresh products that have an irregular or imperfectly axisymmetric shape, which decreases accuracy. To account this issue, many researchers proposed the multiple views method. The classification system for Harum Manis Mango by utilizing additional mirror is developed [3], both top-view and side-view images are used to estimate the volume by the disk method, enabling in-line processing ability. In [30] assumed that the tomato has an ellipsoid and axisymmetric shape, and the volume is computed using the disk method which modeled by conical frustrum, their acquisition system consisted of 5 cameras. Also, in [31], a turntable was used to rotate the strawberry while capturing, a total of 50 captured images in different views are used to reconstruct the 3D shape. However, additional equipment caused even more system complexity, and increased computational time expenses.

In contrast to all the above schemes, we investigated the feasibility of retrieving 3D shapes from shadow, a concept that was introduced in the late 1980s [32–35]. These publications provide information for the reconstruction method and evaluate by measuring simple polygon objects. However, they have only focused on the validity and accuracy of shape recovery.

Our approach focuses on enhancing the speed and accuracy of volume estimation by utilizing simple 2D machine vision while maintaining feasibility within the in-line application process. We present an approach for volume estimation from a single top-view 2D image of the fruit with its shadow. In this research, we used the mango as the test material, which is considered an irregular or axisymmetric shape [3, 23, 24].

This paper is organized into several sections. Section II provides the design of the framework and the light source position calibration method. In Section III, the image processing method and procedure are explained, as well as the 3D reconstruction method. Section IV is an evaluation and discussion of the performance of the developed framework using spherical objects and mangoes. Finally, a conclusion has been provided in Section V.

II. Framework Design and Light Source Calibration

A. Hardware Setup

A simple vision system was designed to capture top-view images of objects, along with their shadows. Fig. 1 illustrates the vision system hardware components. A 5-megapixel USB camera, equipped with a 5–50 mm lens (ELP-USB500W05G-MFV) was mounted on top of the aluminum frame, perpendicular to the fruit being inspected. A typical white color LED SMD (surface mount) type was mounted opposite the camera, projecting light rays to create object shadows at a fixed distance. The angle of the light source was initially adjusted to ensure no shadow fell out of the frame.

B. Software Implementation

The software was implemented as a web application. Fig. 2 shows the graphical user interface (GUI) operated on Google Chrome. The front end of the application was developed using JavaScript, HTML5, and CSS. The backend was developed by micro web framework Flask,

along with the image processing libraries OpenCV and Scikit-Image.

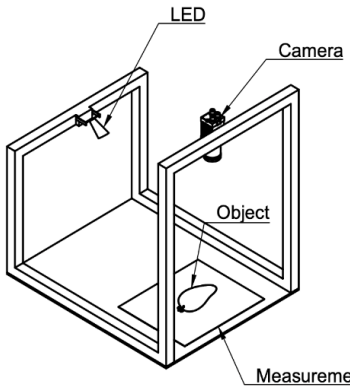

Fig. 1. System hardware component and arrangement.

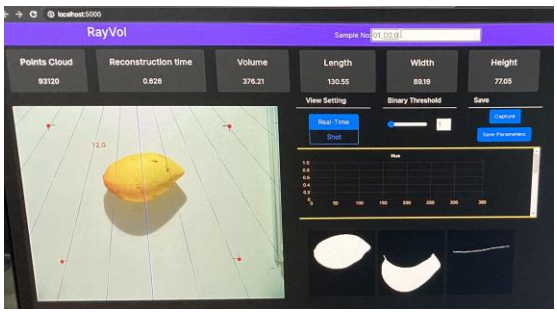

Fig. 2. Graphical user interface of RayVol application.

C. Lightsource Position Calibration

Typically, transformation between image coordinates and world coordinates requires extrinsic and intrinsic matrices, which are derived by performing a calibration. The process usually involves manual labor and taking multiple (10–20) photos of a checkerboard from different angles. Since the shadow and object lie on the same planar surface, a projective transformation called a homography method [36, 37] was used to simplify the process. The relationship between the image plane with pixel data $\mathbf{p}'(x', y', w')$ and world coordinates $\mathbf{p}(x, y, w)$ can be given as (1).

$$\begin{bmatrix} x' \\ y' \\ w' \end{bmatrix} = \begin{bmatrix} h_{11} & h_{12} & h_{13} \\ h_{21} & h_{22} & h_{23} \\ h_{31} & h_{32} & h_{33} \end{bmatrix} \begin{bmatrix} x \\ y \\ w \end{bmatrix} = \mathbf{Hp} \tag{1}$$

where **H** is the homography matrix. All feature points are considered in homogeneous coordinates, thus, $w = w' = 1$. At least four feature points are required to calculate the **H** matrix by the least square method, which is defined from the corners of the measuring area.

The light source position was determined by the intersection of four rays, traced inversely from the shadows cast by the four cuboids of known dimensions, which were arranged in a square formation within the measurement region. Each of cuboid shadow vector AA', BB', CC', and DD' as shown in Fig. 3(a) was used to compute the elevation angle θ as expressed in Eq. (2) for create a ray vector that point to LED light source position,

$$\theta = \tan^{-1}\left(\frac{\text{cuboid height}}{\text{AA'}}\right) \tag{2}$$

Thus, these rays will intersect at a distant point O, which represents the position of the light source. However, since these rays were defined manually, there may be inaccuracies. To account for this, point O is determined from the average of the closest points of intersection of the four rays, as illustrated in Fig. 3(b).

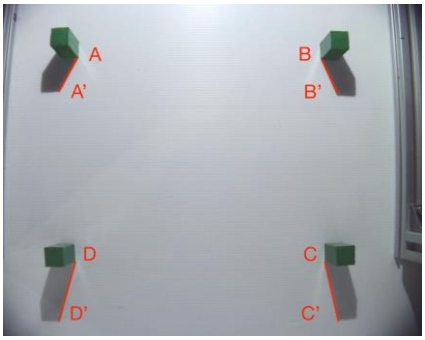

(a)

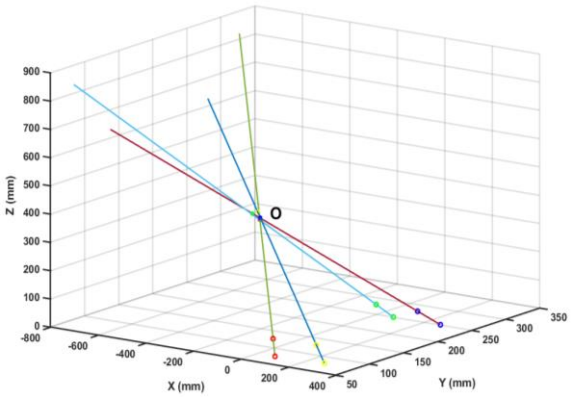

(b)

Fig. 3. Light source calibration process: (a) fixed height cuboid and its shadow cast with originated vector point (A', B', C' and D') and lines (AA', BB', CC', DD). (b) light source position at point O (blue dot) from the nearest average of the closest traced rays.

III. Methods

In this section, the proposed method for 3D volumetric reconstruction from a set of 2D cross-sections (virtual slices) is described. Fig. 4 shows an overview of the processing pipeline. The first step is extracting only the mango and its shadow information from the real-time captured image. To accomplish this, a reference background image obtained during the calibration process is used to perform a simple background subtraction. The resulting image is then subjected to an opening morphological operation to enhance the image and remove any residual noise. Finally, the contouring process is applied to filter out small objects except the largest object, which represents the mango and its shadow. This image results, allowing us to proceed to the next process steps: mango and shadow separation as well as skeleton extraction.

After obtaining the image result, the mango and its shadow were separated by thresholding. This is done by taking advantage of the fact that shadows are in dark areas, while mangoes are colored in bright areas. The Hue-Saturation-Value (HSV) color model was used to separate the brightness contrast by thresholding, where the value channel represents the brightness level. Two binary images of mango and shadow as shown in Fig. 4, served as the inputs for the reconstruction process. Furthermore, during the separation process, the skeleton of the object was also extracted. With the known position of the light source in three-dimensional space, the pixel length between the skeleton image and the bottom edges of shadow image which projected from the light source position was used to determine the object's height data. Cubic spline interpolation was used to generate the point cloud to reconstruct the virtual slice. Finally, the 3D shape was recovered by integration of the virtual slices.

Additionally, a sub-application was also developed in the settings page of the RayVol application, which allows users to manually adjust the Hue-Saturation-Value (HSV) in real-time. This sub-application provides users with an independent threshold for each channel, allowing them to fine-tune to achieve the desired value in real-time and save it as a JSON configuration file, which can be used as a preset for main processing tasks. This feature enhances the system's flexibility and efficiency by enabling users to customize the image processing settings according to their specific needs.

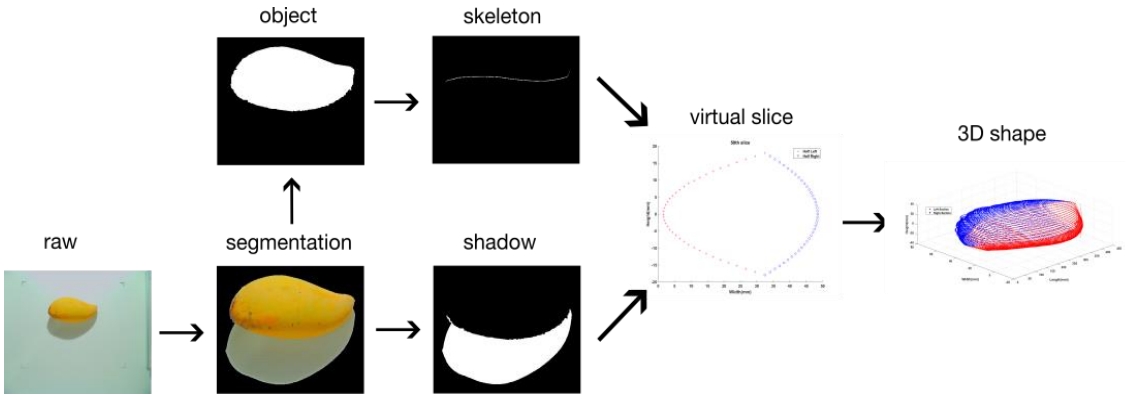

Fig. 4. Overview of the proposed 3D reconstruction pipeline.

A. Virtual Slicing

Reconstructing 3D shapes from a set of 2D cross-sectional slices is widely used in various fields, such as medical imaging, where internal specimen data is obtained using penetration waves generated by techniques such as X-rays or Magnetic Resonance Imaging (MRI). However, these methods can be time-consuming and can contaminate the sample.

In certain applications, particularly for agricultural products, generating 2D cross-sectional profiles must be done non-destructively and as fast as possible. A recent study by [22] introduced a method for producing virtual slices of cucumber from 2D photographs. This was achieved by circulating around the object's midline if the cucumber's shape closely resembles that of a simple cylinder.

Our proposed methodology employs cubic spline interpolation to create point clouds from boundary object information which extracted from 2D images, in combination with height data obtained through shadow casting. This approach enables the precise and dependable two-dimensional cross-sectional slices reconstruction for both regular and irregular shapes of agricultural material, which enhances the quality of reconstructions.

The process of generating the virtual slicing involves dividing the object into two halves. Each of the halves is then constructed using three points as basis points, which are illustrated in Fig. 5(b) and Fig. 5(c). The first basis point is located at the boundary of the object image and constructed at zero on the *z*-axis (height axis). The second basis point is obtained through the shadow casting method, at the positive *z*-axis, which derived from the height data using Eq. (3). The obtained height h data must be divided in half to generate the third point in the subsequent process.

$$h = \frac{s\tan(\theta)}{2} \tag{3}$$

The length of the resulting shadow s is determined by the displacement of the object's medial information and the bottom boundary of the shadow image which relative to the position of the light source, as illustrated in Fig. 5(a) and Fig. 5(b).

The object's medial information is obtained by performing skeletonization of the object image. To determine the θ angle, the inverse trigonometry Eq. (4) is utilized.

$$\theta = \cos^{-1}\left(\frac{w}{v}\right) \tag{4}$$

where w and v are displacements from B to C and A to C respectively. The third point in the negative *z*-axis is generated by applying a mirroring transformation from the second point in the positive z-axis This methodology assumes that most agricultural objects have an axi-

symmetric configuration, despite any inherent irregularities. Finally, this set of three points is used to construct new points through cubic spline interpolation as shown in Fig. 5(d).

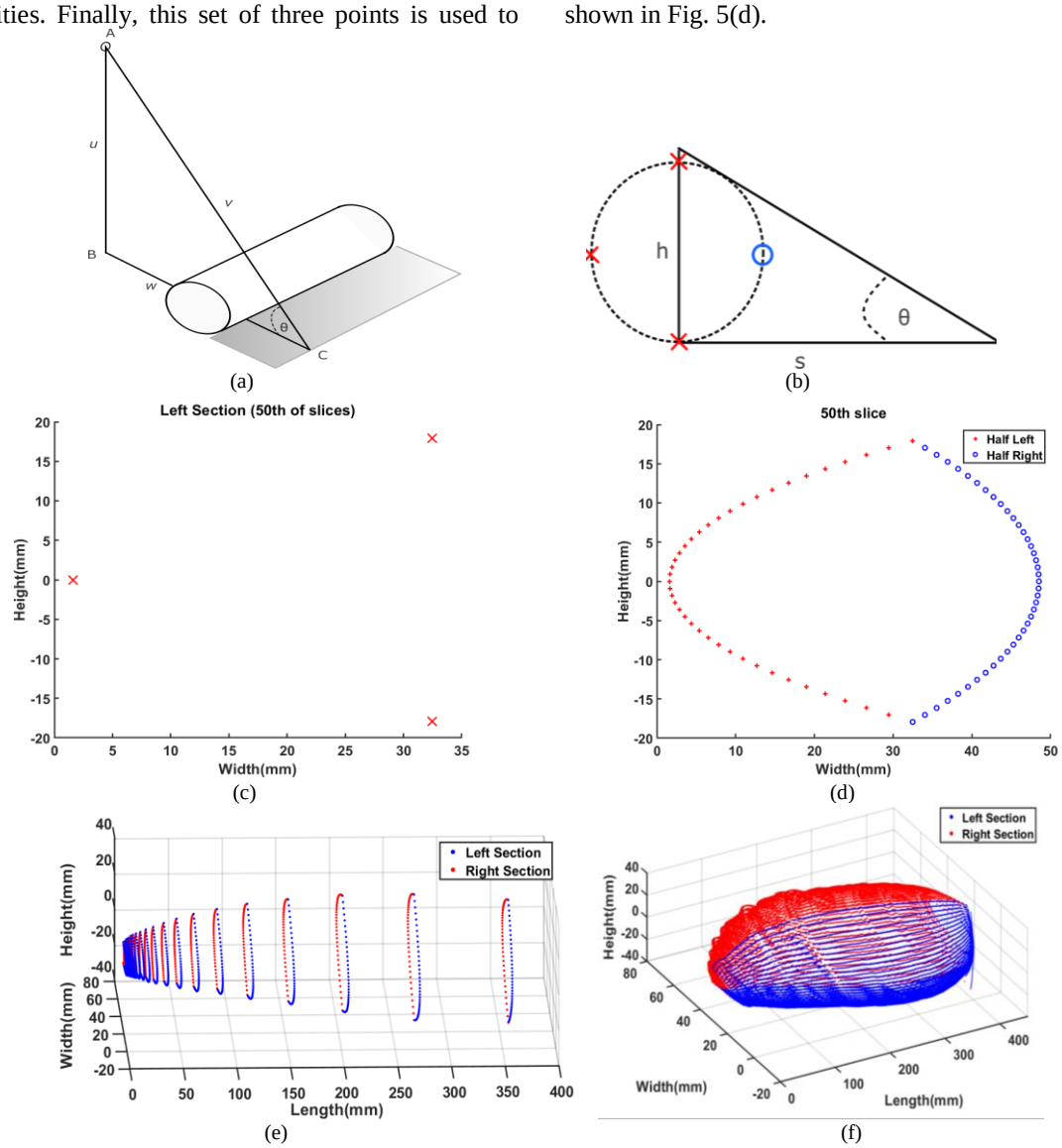

Fig. 5. 3D reconstruction process: (a) and (b) visualizing the geometry structure relationship of shadow casting in 3D and 2D, respectively; (c) obtaining an example of the left half of the virtual slice through the shadow casting method, as indicated by the symbol "x" in (b); (d) the completed virtual slice by combining the left and right halves; (e) Visualizing of the virtual slice stacking along x-axis; and (f) Fully 3D reconstruction.

B. Volumemetric Rendering

To reconstruct a 3D volume image, the reconstructed slices are stacked sequentially along the x-axis as shown in Fig. 5(e), with a pixel length distance of one, which is transformed to real-world information by performing a homography transform. Fig.5 (f) illustrates the completed 3D reconstruction obtained from a stack of virtual slices. To estimate the volume, the finite sum approximation of an integral is utilized, expressed as

$$V = \sum_{i=1}^{n} A(x_i)\Delta x \tag{5}$$

where Δx is stack distance in world coordinate and $A(x_i)$ represents the area of the closed polygon of the individual full slice, which is approximated by the Shoelace method.

IV. Results and Discussion

A. Repeatability

The repeatability of the proposed system was evaluated using three metal spheres of different sizes. The volume of each individual sphere was computed using the sphere volume formula:

$$V = \frac{4}{3}\pi r^3 \tag{6}$$

where r is radius of the sphere. The volumes for the three spheres were calculated to be 28.73 cm^3, 65.45 cm^3, and 268.1 cm^3, respectively.

Thirty measurements were taken for each sphere at the same location in the measurement area using the proposed system. The precision of the system for volume estimation was evaluated by determining the coefficient

of variation [38] which is calculated from Eq. (7) for the estimated volume using the proposed system was 0.88%, 0.65%, and 0.82% for the three different-sized spheres, respectively as shown in Table I. Our volume estimation method demonstrated high repeatability; the CV is less than 1% for all samples.

$$CV = (\sigma / \mu) \times 100\% \quad (7)$$

TABLE I: VARIATION ANALYSIS OF THE VOLUME OF A SPHERE METAL BALLS MEASURED BY RAYVOL

Size (mm)	*n*	Mean (μ)	S.D. (σ)	CV (%)
38	30	30.14	0.267	0.88
50	30	67.68	0.43	0.65
80	30	273.13	2.23	0.82

B. Accuracy

The comparison was performed between the results measured by the proposed machine vision system and the water displacement method based on Archimedes' principle. The thirty mangoes were used as samples, randomly selected from a local farm. The sample was positioned in the measurement area, similarly to the repeatability evaluation procedure. The results obtained from the proposed method were compared with the water displacement method. The deviation is shown in Fig. 6(a), indicating that almost all the errors from the proposed method fell within the 95% limit of agreement.

Fig. 6(b) shows the comparison data, revealing a significant linear correlation between the volume estimated from RayVol framework and the volume measured by Water Displacement Method (WDM). The squared correlation coefficient (R^2) between the water displacement method and the RayVol measurement was 0.9849. This value signifies the proportion of the variance in the RayVol measurements that can be explained by the variance in the actual measurements. A higher R^2 value implies a closer correspondence between the RayVol measurements and the actual measurements, thereby indicating the greater accuracy and reliability of the proposed machine vision system.

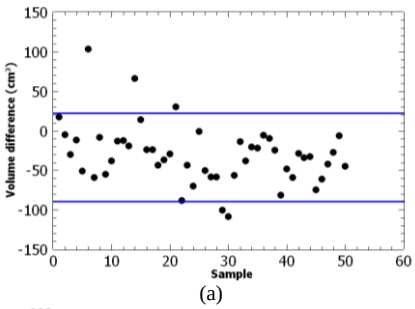

(a)

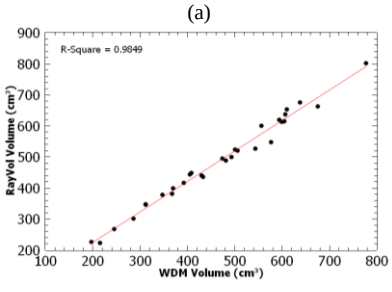

(b)

Fig. 6. The deviation and accuracy performance between water displacement method and RayVol framework: (a) 1.96-σ plot for volume difference; (b) R^2 and correlation.

C. Mango Size Classification Experiment

In this study, the proposed framework was utilized for mango size classification. A total of thirty mangoes were selected and categorized based on the assigned codes, as shown in Table II. The classification results were visually represented through box plots, as shown in Fig. 7. Each box plot contained the dataset, where the center of the box represented the median, the box edges represented the 25th and 75th quartiles, the whiskers illustrated the 5th and 95th quartiles, and the minimum and maximum values were presented as outliers.

TABLE II: VARIATION ANALYSIS OF THE VOLUME OF A SPHERE METAL BALLS MEASURED BY RAYVOL

Type	Code	Volume (cm³)
Small	S	180–234
Medium	M	235–315
Large	L	316–450

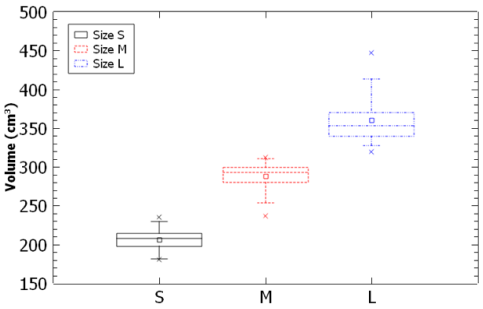

Fig. 7. Box plot representation of mango classification by volume. Showing the quartiles, the 5th and 95th percentiles (whiskers) and extreme values to the minimum and maximum.

D. Computation Expense

The PC computer with an AMD Ryzen 7 5700 (3.8 GHz) was used as the computational device for this research. The Python backend software and web application were operated on Ubuntu 16.04. The computational time of all experiments ranged from 0.3 to 0.75 s, generating 28,000–40,000 points clouds. The setup was able to estimate the object volume for 1–3 objects per second with an object volume ranging from 180–480 cm^3 and a resolution of 28,000–40,000 points cloud.

The computation time varied depending on the size of the image and the size of the object being processed. To improve the computation time, the camera resolution could be reduced. However, reducing the camera resolution would also affect the quantity of the point cloud, which might impact the resolution of the volume estimation. Therefore, it is essential to consider the trade-off between computation time and volume estimation resolution when selecting the camera resolution.

V. CONCLUSION

A simple and non-contact framework for measuring the volume of axi-symmetrical objects based on shadow casting is presented. A cost-effective machine vision framework based on this method was designed and built specifically for measuring agricultural materials. The

reconstruction of a 3D model and estimation of volume is fast with a single captured image, making it suitable for an inline process.

The precision of the proposed method was demonstrated with the Coefficient of Variation (CV) which was less than 1% for all of three spheres. whereas the accuracy was determined by the coefficient of determination (R^2) between the Water Displacement Method (WDM) and proposed method which was 0.9849. Furthermore, the computation time varied between 0.3 to 0.75 s with generating 28,000-40,000 points clouds per object.

The results of the performance analysis have shown that the proposed framework is accurate, precise with non-destructive for measuring the volume of axi-symmetrical objects, particularly in the case of agricultural materials. However, the resolution of volume measurements is dependent on the size of the region of interest in the image, which is also related to the size of the object being measured, and this may affect computation time. Furthermore, the angle of the light source also has an impact on accuracy. The setting up of the light source must be carefully done. Nevertheless, the proposed system provides sufficient accuracy and precision to make it competitive in this research area and in industrial applications.

CONFLICT OF INTEREST

The authors declare no conflict of interest.

AUTHOR CONTRIBUTIONS

S.S. and T.S.: methodology, S.S.: software, S.S. and T.S.; validation, T.S. and N.N.: formal analysis, S.S. and T.S.: investigation, S.S. and T.S.: resources, S.S. and T.S.: writing-original draft preparation, N.N.: writing-review and editing, S.S. and T.S.: visualization, T.S. and N.N.: supervision.

REFERENCES

[1] Y. Wang and Y. Chen, "Fruit morphological measurement based on three-dimensional reconstruction," *Agronomy*, vol. 10, no. 4, #455, Mar. 2020

[2] T. Huynh, L. Tran, and S. Dao, "Real-time size and mass estimation of slender axi-symmetric fruit/vegetable using a single top view image," *Sensors*, vol. 20, no. 18, #5406, Sep. 2020.

[3] M. F. Ibrahim, F. S. Ahmad Sa'ad, A. Zakaria, and A. Y. Md Shakaff, "In-line sorting of Harumanis mango based on external quality using visible imaging," *Sensors*, vol. 16, no. 11, #1753 Nov. 2016.

[4] N. K. Mahanti *et al*., "Emerging non-destructive imaging techniques for fruit damage detection: Image processing and analysis," *Trends in Food Science & Technology*, vol. 120, pp. 418–438, Feb. 2022

[5] I. Torigoe and Y. Ishii, "Acoustic bridge volumeter," *Trans. of the Society of Instrument and Control Engineers*, vol. 30, no. 11, pp. 1303–1309, 1994.

[6] T. Kobata, M. Ueki, A. Ooiwa, and Y. Ishii, "Measurement of the volume of weights using an acoustic volumeter and the reliability of such measurement," *Metrologia*, vol. 41, no. 2, pp. S75–S83, Apr. 2004.

[7] M. Ueki, T. Kobata, K. Ueda, and A. Ooiwa, "Measurements of the volume of weights from 1 g to 50 g using an acoustic volumeter," in *Proc. SICE Annual Conference 2005 in Okayama*, Japan, 2005, pp. 1742–1744.

[8] V. A. Sydoruk, J. Kochs, D. Dusschoten, G. Huber, and S. Jahnke, "Precise volumetric measurements of any shaped objects with a novel acoustic volumeter," *Sensors (Basel)*, vol. 20, no. 3, #760, Jan. 2020.

[9] D.-W Sun, *Computer Vision Technology for Food Quality Evaluation (Second Edition)*, Academic Press, 2016.

[10] B. Zhang, N. Guo, J. Huang, B. Gu, and J. Zhou, "Computer vision estimation of the volume and weight of apples by using 3D reconstruction and noncontact measuring methods," *Journal of Sensors*, vol. 2020, #5053407, Nov. 2020.

[11] A. Anders, D. Choszcz, P. Markowski *et al*., "Numerical modeling of the shape of agricultural products on the example of cucumber fruits," *Sustainability*, *vol.* 11, no. 10, #2798, 2019.

[12] V. Riffo and R. Hidalgo, "Active inspection of objects to detect possible damage and measure their volume using 3D reconstruction," *Measurement*, vol. 199, #111541, Aug. 2022

[13] Z. Cai, C. Jin, J. Xu, and T. Yang, "Measurement of potato volume with laser triangulation and three-dimensional reconstruction," *IEEE Access*, vol. 8, pp. 176565–176574, 2020

[14] Q. Su, N. Kondo, M. Li, H. Sun, D. F. Al Riza, and H. Habaragamuwa, "Potato quality grading based on machine vision and 3D shape analysis," *Computers and Electronics in Agriculture*, vol. 152, pp. 261–268, Sep. 2018.

[15] Q. Su, N. Kondo, M. Li, H. Sun, and D. F. Al Riza, "Potato feature prediction based on machine vision and 3D model rebuilding," *Computers and Electronics in Agriculture*, vol. 137, pp. 41–51, May 2017.

[16] F. Alkhawaja, M. Jaradat, and L. Romdhane, "Techniques of indoor positioning systems (IPS): A survey," presented at 2019 Advances in Science and Engineering Technology International Conferences, Dubai, United Arab Emirates, Mar. 2019.

[17] I. Nyalala, C. Okinda, L. Nyalala *et al*., "Tomato volume and mass estimation using computer vision and machine learning algorithms: Cherry tomato model," *Journal of Food Engineering*, vol. 263, pp. 288–298, Dec. 2019.

[18] G. Vivek Venkatesh, S. Md. Iqbal, A. Gopal, and D. Ganesan, "Estimation of volume and mass of axi-symmetric fruits using image processing technique," *International Journal of Food Properties*, vol. 18, no. 3, pp. 608–626, Mar. 2015.

[19] F. S. A. Sa'ad, M. F. Ibrahim, A. Y. Md. Shakaff, A. Zakaria, and M. Z. Abdullah, "Shape and weight grading of mangoes using visible imaging," *Computers and Electronics in Agriculture*, vol. 115, pp. 51–56, Jul. 2015.

[20] L. Wang, P. Shi, L. Chen, J. Gielis, and K. J. Niklas, "Evidence that Chinese white olive (Canarium album (Lour.) DC.) fruits are solids of revolution," *Botany Letters*, Jul. 2023. doi: 10.1080/23818107.2023.2238020

[21] N. Nunak and T. Suesut. "Measuring geometric mean diameter of fruits and vegetables using light sectioning method," *Songklanakarin Journal of Science and Technology*, vol. 31, no. 6, pp. 629–633, 2009.

[22] A. Soleimanipour and G. R. Chegini, "Three-dimensional reconstruction of cucumbers using a 2D computer vision system," *Food Measure*, vol. 13, pp. 571–578, Mar. 2019.

[23] W. Spreer and J. Müller, "Estimating the mass of mango fruit (Mangifera indica, cv. Chok Anan) from its geometric dimensions by optical measurement," *Computers and Electronics in Agriculture*, vol. 75, no. 1, pp. 125–131, Jan. 2011.

[24] W. Aung, T. T. Thu, H. T. D. Aye, P. P. Htun, and N. Z. Aung, "Weight estimation of mango from single visible fruit surface using computer vision," in *Proc. 2020 59th Annual Conference of the Society of Instrument and Control Engineers of Japan (SICE)*, Sep. 2020, pp. 366–371.

[25] J. Siswantoro and E. Asmawati, "A new framework for measuring volume of axisymmetric food products using computer vision system based on cubic spline interpolation," in *Proc. 2016 2nd Int. Conf. on Science in Information Technology*, Balikpapan, Indonesia, 2016, pp. 74–78.

[26] H. M. Tran, K. T. Pham, T. M. Vo, T.-H. Le, T. T. M. Huynh, and S. V. T. Dao, "A new approach for estimation of physical properties of irregular shape fruit," *IEEE Access*, vol. 11, pp. 46550–46560, 2023.

[27] T. T. M. Huynh, L. TonThat, and S. V. T. Dao, "A vision-based method to estimate volume and mass of fruit/vegetable: Case study of sweet potato," *International Journal of Food Properties*, vol. 25, no. 1, pp. 717–732, Dec. 2022.

[28] T. Mon and N. ZarAung, "Vision based volume estimation method for automatic mango grading system," *Biosystems Engineering*, vol. 198, pp. 338–349, Oct. 2020
[29] H. Yin, W. Yi, and D. Hu, "Computer vision and machine learning applied in the mushroom industry: A critical review," *Computers and Electronics in Agriculture*, vol. 198, #107015, Jul. 2022.
[30] S. Uluisik, F. Yildiz, and A. T. Ozdemir, "Image processing based machine vision system for tomato volume estimation," in *Proc. 2018 Electric Electronics, Computer Science, Biomedical Engineerings Meeting*, Istanbul, Apr. 2018, pp. 1–4.
[31] B. Li, H. M. Cockerton, A. W. Johnson *et al*., "Defining strawberry shape uniformity using 3D imaging and genetic mapping," *Hortic Res*, vol. 7, no. 1, #115, Dec. 2020
[32] M. Adjouadi and J. T. Tou, "Shadow analysis in scene interpretation," in *Proc. the 4th Scandinavian Conference*, Trondheim, Norway, 1985, pp. 821–829.
[33] John R. Kender and Earl M. Smith, "Shape from darkness: deriving surface information from dynamic shadows," in *Proc. the Fifth AAAI National Conference on Artificial Intelligence*, 1986, pp. 664–667.
[34] L. Cavanagh and Y. G. Leclerc, "Shape from shadows," *Journal of Experimental Psychology: Human Perception and Performance*, vol. 15, no. 1, pp. 3–27, 1989.
[35] T. P. Seng, G. W. Leng, and C. K. Luk, "Shape reconstruction from shadow and shading," in *Proc. IECON '93 - 19th Annual Conference of IEEE Industrial Electronics*, Maui, HI, USA, 1993, pp. 1639–1644.
[36] S. Gulphanich, N. Nunak, and T. Suesut, "3D inspection for HDD production process using laser light sectioning," presented at the International MultiConference of Engineers and Computer Scientists, Hong Kong, 2015.
[37] S. Sukprasertchai, S. Wangthong and P. Iamraksa, "Navigation and maneuvering investigation system based on infrared camera," presented at the International Offshore and Polar Engineering Conference, Sapporo, 2018.
[38] L. Dah-Jye, X. Xu, J. Eifert, and P. Zhan, "Area and volume measurements of objects with irregular shapes using multiple silhouettes," *Optical Engineering*, vol. 45, Feb. 2006. doi: 10.1117/1.2166847

Copyright © 2024 by the authors. This is an open access article distributed under the Creative Commons Attribution License (CC BY-NC-ND 4.0), which permits use, distribution and reproduction in any medium, provided that the article is properly cited, the use is non-commercial and no modifications or adaptations are made.

Siwakorn Sukprasertchai received the B.S. degree in applied physics and M.Eng. in instrumentation engineering from the King Mongkut's Institute of Technology Ladkrabang, Bangkok, Thailand. He is pursuing his doctoral degree in electrical engineering at school of engineering, King Mongkut's Institute of Technology Ladkrabang, Bangkok, Thailand. His current research interests include computer vision, 3D reconstruction, and metric vision.

Taweepol Suesut received the B.Eng. degree in instrumentation engineering from King Mongkut's Institute of Technology Ladkrabang and the M.Eng. degree in electrical engineering from the same university and Ph.D. degree in automation engineering from University of Leoben, Austria. He is an associate professor in the Department of Instrumentation and Control engineering. His area of interest is instrumentation system design and automation in food factories, especially machine vision for measurement and inspection as well as infrared-thermography.

Navaphattra Nunak received the B.Eng. degree in Food engineering from King Mongkut's Institute of Technology Ladkrabang and the M.Eng. degree in Post-Harvest and Food Process Engineering from Asian Institute of Technology and Dr. degree at University of Natural Resources and Life Sciences, Vienna, Austria. She is an associate professor in the Department of Food Engineering. Her area of interest is measurement and instruments in food processing, hygienic engineering and Infrared thermography.